Diffusion-weighted MRI of abscess formations in children and young adults

Henning Neubauer, Isabel Platzer, Verena Rabea Mueller, Thomas Meyer, Johannes Liese, Herbert Koestler, Dietbert Hahn, Meinrad Beer

Wuerzburg, Germany

Background: **Diffusion-weighted MRI (DWI) is helpful for detection of brain abscess and pelvic abscess in adults. In the present study, we evaluated the diagnostic performance of DWI in children and young adults with abdominal and soft tissue abscess formations.**

Methods: **Seventeen patients (11 females, aged 13 ± 6 years) with suspected abdominal or soft-tissue abscess underwent routine MRI including free-breathing DWI and contrast-enhanced T1w imaging. Seventeen random age-matched patients with non-purulent abdominal fluid collections served as controls. Mean apparent diffusion coefficent (ADC) was measured for abscess, muscle, liver, spleen and kidney tissue as well as for cerebrospinal fluid, urine and free abdominal fluid.**

Results: **All fluid collections were identified on diffusion-weighted images. Thirteen of 14 confirmed abscess formations showed an ADC < 1.0×10^{-3} mm^2/s with a mean value of 0.80 ± 0.38 mm^2/s. One tuberculous soft-tissue abscess had a higher ADC of 1.85×10^{-3} mm^2/s. Ring enhancement on T1w imaging was seen in three non-purulent fluid collections. There were no false-positive findings in the control group.**

Conclusions: **Diffusion-weighted MRI is highly sensitive for abscess and may add specificity to contrast-enhanced T1w imaging of ring-enhancing fluid collections. DWI with free-breathing rapid image acquisition and without the need of intravenous contrast application constitutes a particularly useful choice in pediatric imaging.**

World J Pediatr 2012;8(3):229-234

Key words: **abscess;**
contrast medium;
diffusion-weighted imaging;
magnetic resonance imaging;
pediatric

Author Affiliations: Institute of Radiology, Department of Pediatric Radiology, University Hospital Wuerzburg, Josef-Schneider-Straße 2, 97080 Wuerzburg, Germany (Neubauer H, Platzer I, Beer M); Department of Pediatrics, University Hospital Wuerzburg, Josef-Schneider-Straße 2, 97080 Wuerzburg, Germany (Mueller V, Liese J); Pediatric Surgery Unit, Department of Surgery, University Hospital Wuerzburg, Oberduerrbacher Str. 6, 97080 Wuerzburg, Germany (Meyer T); Institute of Radiology, University Hospital Wuerzburg, Oberduerrbacher Str. 6, 97080 Wuerzburg, Germany (Koestler H, Hahn D)

Corresponding Author: Henning Neubauer, MD, MBA, Institute of Radiology, Department of Pediatric Radiology, University Hospital Wuerzburg, Josef-Schneider-Straße 2, 97080 Wuerzburg, Germany (Tel: 0049-931-201-34715; Fax: 0049-931-201-34857; Email: neubauer@roentgen.uni-wuerzburg.de)

doi: 10.1007/s12519-012-0362-4

Original article

Introduction

Since the mid-1990s, diffusion-weighted MRI (DWI) has been established as a valuable tool in neuroimaging for detection of acute cerebral ischemia[1] and, more recently, of intracranial neoplasm and abscess formation.[1,2] DWI visualises the varying degree of Brownian diffusion in biological tissues[3] and facilitates the detection of restricted diffusion and differentiation between tissues of different cellular density and water content. Recently, a number of extracranial applications of DWI have been studied, including the detection and prognostic evaluation of malignant tumors,[4] differentiation between malignant and non-malignant lymphnodes[5] and detection of chronic inflammatory bowel disease in adults.[6] To date, there are only few published studies on extracranial DWI in pediatric patients.[7,8]

Purulent fluid collections within the abdominal cavity or soft-tissue structures usually require surgical or interventional emergency treatment. MRI presently depends on intravenous gadolinium-containing contrast agent for differentiation of abscess from non-purulent fluid collection based on the diagnostic criterion of ring enhancement. DWI can diagnose both cerebral and abdominal abscess formations with high accuracy in adults.[2,9] Rapid image acquisition in free-breathing technique and reliable abscess detection without the need of intravenous contrast medium, as with DWI, would be a particularly welcome extension to standard scanning protocols in pediatric imaging. We therefore assessed the detectability and imaging characteristics

of purulent fluid collections on DWI in a group of pediatric patients and young adults.

Methods

The present study was based on the retrospective analysis of data from 17 consecutive patients (11 females) with a mean age of 13 ± 6 years (range: 12 months to 20 years) who had been examined over a two-year period between August 2009 and 2011. The study was conducted in accordance with the *Declaration of Helsinki* 1964. All patients were referred to routine MRI for clinically and/or sonographically suspected abscess. Informed written consent was obtained from all patients and/or their parents. Clinical details are outlined in Table 1. Fourteen patients subsequently underwent surgical treatment at our institution, immediately after MRI (n=4) or over the ensuing days (range: 0-13 days after MRI, median: 1 day). Surgical and histopathological/microbiological correlation was available for all these patients. Two patients recovered after conservative treatment and were discharged without further MR imaging. One patient with suspected abscess secondary to acute appendicitis received treatment at another institution and was lost to follow-up.

MRI examination required sedation in three patients aged 1 to 4 years. All MRI examinations were performed as routine diagnostic imaging studies with a 1.5 Tesla Magnetom Symphony (n=8), a 1.5 Tesla Magnetom Avanto (n=7) and a 3 Tesla Magnetom Skyra scanner (n=2), all Siemens Medical, Germany, with commercially available coils. In addition to T1- and T2-weighted imaging and contrast-enhanced sequences, as appropriate, free-breathing diffusion-weighted single-shot echo-planar imaging (SS-DW-EPI) with diffusion-sensitizing gradients applied sequentially along the three orthogonal directions was acquired with the following scanning parameters. We used one DWI sequence with a large field of view (FOV) for abdominal imaging (b-values 50 and 800 s/mm^2, TR 9000 ms, TE 126 ms, 8 averages, epi factor 128, fat saturation, slice thickness 6 mm, base resolution 128, FOV 360 mm, voxel size 2.8×2.8×6.0 mm, scanning time for 40 slices 7 minutes 21 seconds) and another with a smaller FOV for head/neck and extremitites (b-values 0-50 and 800-1000 s/mm^2, TR 4600 ms, TE 137 ms, 2 to 6 averages, epi factor 128, fat saturation, slice thickness 6 mm, base resolution 128, FOV 230 mm, voxel size 1.8×1.8×6.0 mm, scanning time for 19 slices 41s to 2 min 55s).

Diffusion-weighted (DW) isotropic images obtained at high b-values were used for abscess detection. Areas of restricted diffusion, e.g., in hypoxic brain tissue, in tumour with high cellular density or abscess, are depicted with high signal intensity at high b-values (Fig. 1). Quantitative measurement of the apparent diffusion coefficient (ADC) was performed with region of interest (ROI) techniques on automatically generated ADC maps for all abscess formations as well as, if contained within the scanning volume, for skeletal muscle, cerebrospinal fluid, liver and spleen tissue, renal cortex, free abdominal fluid and finally for the fluid signal of the renal pelvis and the urinary bladder. Mean ADC was recorded from all ROI measurements. In the present study, detectability, size and signal intensity of all lesions on DWI were determined by one board-certified radiologist with 3 years of experience in extra-cranial DWI, blinded to clinical information. Analyses were performed separately for DWI and conventional MRI sequences within 7 days.

From our pool of routine clinical MRI studies, we chose a random control sample of 17 age-matched patients who had had an abdominal DWI study and some degree of free fluid in the abdominal cavity. All control patients had been imaged for suspected abdominal pathologies other than abscess and none of these patients had fluid collections with ring enhancement. All these examinations were performed with the same scanner hardware (Magnetom Symphony n=10, Magnetom

Table 1. Mean apparent diffusion coefficient (ADC) of various tissues and fluids measured in study patients and controls

	n	Mean ADC values, × 10^{-3} mm^2/s				
		Mean	Median	Standard deviation	Minimum	Maximum
Abscess*	13	0.80	0.78	0.38	0.37	1.86
Muscle	24	1.19	1.25	0.18	0.71	1.38
Liver	17	1.13	1.09	0.12	1.02	1.42
Spleen	13	0.88	0.86	0.07	0.76	0.98
Renal cortex	21	1.80	1.79	0.20	1.40	2.11
Renal pelvis	16	3.17	3.15	0.16	2.89	3.59
Free abdominal fluid	26	3.19	3.21	0.29	2.70	3.79
Urinary bladder	26	3.14	3.12	0.20	2.87	3.65
Cerebrospinal fluid	28	3.51	3.53	0.24	3.05	3.87

*: only confirmed cases of abscess formation (n=13), excluding patients no. 2, 5, 13 and 15.

Avanto *n*=7) and with the scanning protocols described. ADC measurements in the controls were performed with the same methods as in the study patients.

Fusion of T2 HASTE images with diffusion-weighted images (Fig. 2) was performed with commercially available software (3D image fusion, Siemens Medical, Erlangen, Germany).

Statistical analysis

Normally distributed data were presented as mean ± SD. Between the groups comparison was performed with the independent sample *t* test for variables following normal distribution and the Mann-Whitney *U* test for variables deviating from normal distribution. For analysis of differences in lesion size, the difference of the longest transversal lesion diameter on DWI and T1 post-contrast images was tested with a one-sample *t* test against *a* test value of zero. Receiver operating curve (ROC) analysis (nonparametric assumption, null hypothesis: true area = 0.5) was used to study the diagnostic performance of

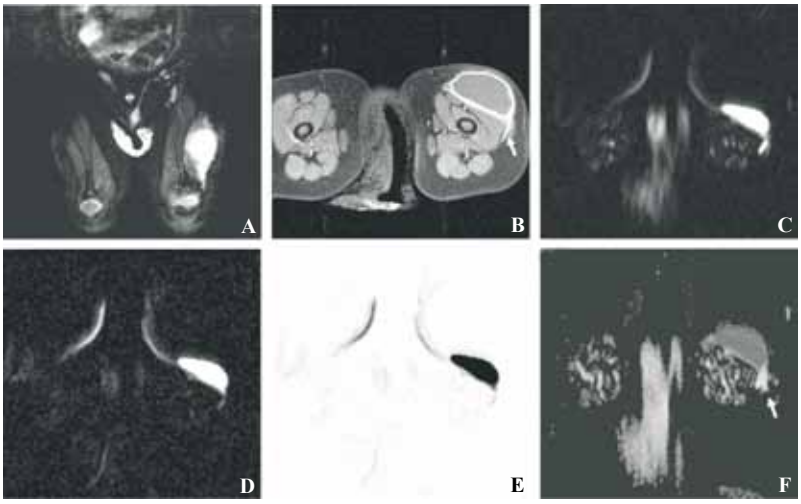

Fig. 1. Patient 6, sterile chronic post-vaccinational soft tissue abscess on the left upper leg of a 12-month old boy [coronal T2 TIRM (**A**), transversal post-contrast T1 TSE FS (**B**), DWI b=0 (**C**), DWI b=1000 (**D**), DWI b=1000 inverted gray-scale (**E**), ADC map (**F**)]. The abscess shows bright fluid signal on T2 TIRM (**A**) and strong peripheral contrast enhancement on T1w (**B**). High signal intensity on DWI with high b-value, equaling restricted diffusion, is seen within the abscess (**D**, **E**). Mean ADC was 0.78 $\times 10^{-3}$ mm^2/s. There is perifocal inflammatory contrast enhancement adjacent to the lateral abscess contour (arrow, **B**), which appears in bright gray on the ADC map (arrow, **F**) with a mean ADC of 1.6 $\times 10^{-3}$ mm^2/s, suggestive of oedematous soft tissue.

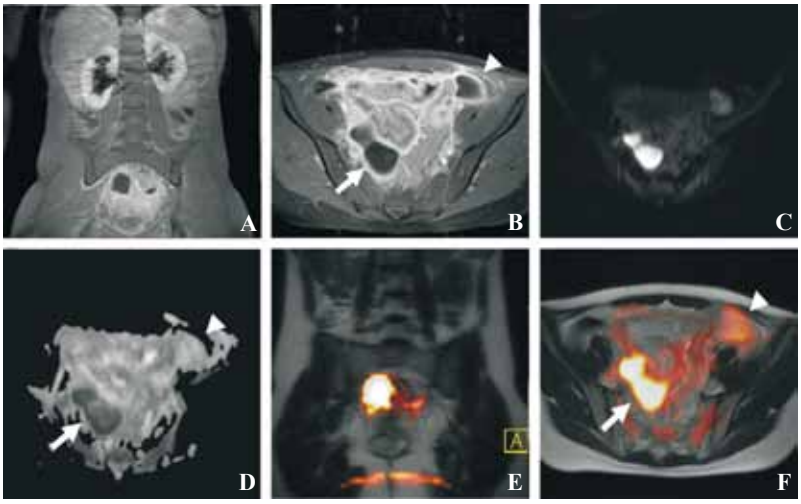

Fig. 2. Patient 11, diffuse peritonitis in the lower abdomen secondary to perforated appendicitis. Two ring-enhancing lesions are discernable (arrow, arrowhead). DWI differentiates between the posteriorly located abscess (arrow, ADC 0.76 × 10^{-3} mm^2/s) and the anterior non-purulent collection (arrowhead, ADC 2.45 × 10^{-3} mm^2/s), as confirmed by surgery. Coronal (**A**) and transversal (**B**) post-contrast T1 TSE FS, transversal DWI b=800 (**C**), ADC map (**D**), 3D image fusion of corresponding coronal (**E**) and transversal (**F**) T2 HASTE with colourised half-transparent overlay of transversal DWI b=800.

Table 2. Descriptives of study patients, lesion localization, mean ADC value of the target fluid collection, treatment and diagnosis

Patient no.	Sex	Age y	Lesion localization	Leukocyte count, $\times 10^3/\mu L$	CRP, mg/dL	ADC value, $\times 10^{-3}$ mm^2/s	Therapy	Surgical treatment days post-MRI	Final diagnosis
1	F	8	proximal tibial metaphysis	8.2	0.26	0.86	surgery	2	Brodie abscess, positive for *Staphylococcus aureus*
2	M	14	lower leg	**14.3**	0.35	1.84	surgery	1	Super-infected seroma after lower leg amputation secondary to osteosaroma, positive for *Streptococcus G*
3	M	15	hip joint	11.2	**8.7**	1.86	surgery	1	Curschmann-Steinert syndrome, tuberculous coxarthritis and suppurative periarthritis
4	M	18	para-pharyngeal	**10.7**	**8**	0.45	surgery	0	Cervical abscess secondary to bilateral chronic tonsillitis
5	M	10	knee joint	7.6	**3.8**	2.15	surgery	13	Suspected recurrent empyema two weeks after surgical treatment of joint empyema, no recurrence noticed on repeated arthroscopy
6	M	1	upper leg	11.5	0.05	0.78	surgery	1	Chronical post-vaccinational soft-tissue abcess
7	F	4	cervical	12.1	**0.79**	0.38	surgery	1	Recurrent suppurative lymphadenitis, suspected MOTT, negative on microbiological analysis
8	F	10	cervical	**17.3**	**15.1**	0.88	surgery	0	Parapharyngeal abscess
9	F	20	abdominal	**10.4**	**9.1**	0.61	surgery	5	Primary manifestation of Crohn's disease, confirmed after ileocoecal resection
10	F	18	abdominal	10	**14.9**	0.78	surgery	0	Perforated appendicitis
11	F	14	abdominal	11.4	**32.6**	0.76	surgery	0	Perforated appendicitis
12	M	16	abdominal	**20.7**	**25.7**	0.85	surgery	4	Crohn's disease, inflammatory conglomerate
13	F	16	abdominal	-	-	0.85	lost to follow-up	-	Suspected perforated appendicitis
14	F	17	abdominal	7.6	0.2	0.37	conservative	-	Recurrent residual Douglas abcess after surgical abscess lavage and drainage secondary to perforated appendicitis
15	F	10	abdominal	2.4	0.3	3.05	surgery	2	Encapsulated pelvic fluid collection, intraoperative assessment: no abscess
16	F	4	abdominal	8.4	**1.45**	0.77	surgery	1	Currarino syndrome, subphrenic abscess
17	F	19	renal	5.5	**11.2**	0.95	conservative	-	Suppurative pyelonephritis

F: female; M: male; MOTT: mycobacterium other than tuberculosis; ADC: apparent diffusion coefficient. Values of leukocyte count and c-reactive protein (CRP) beyond the reference range in bold letters.

ADC values. A P value <0.05 was considered statistically significant. Analyses were performed with the PASW (SPSS) Statistics 18 software package (SPSS Inc., Chicago, USA).

Results

Mean ADC values for selected anatomical regions and fluid collections are listed in Table 1. No statistically significant difference was found for mean ADC values between patients and controls or between studies performed on the Magnetom Symphony and the Magnetom Avanto scanner (independent sample t test, all P>0.05).

Descriptives and final diagnosis of all 17 study patients are listed in Table 2. All patients and controls showed fluid collections on T1w and T2w imaging. Image quality was generally good, only two examinations suffered from motion artifacts. All fluid collections were identified on the diffusion-weighted sequences. Marked susceptibility and distortion artifacts were seen in 3 patients; however, the lesions of interest were nevertheless clearly visible and sufficiently delineated for analytic measurement. Size of the registered fluid collections ranged between 7 and 52 mm (DWI), compared to 5 and 54 mm (T1w post-contrast), with a mean size of 26 ± 15 mm (DWI) and 26 ± 16 mm (T1w post-contrast). The mean difference of lesion size on DWI and T1w post-contrast images was not significantly different from zero (P=0.660).

ADC values of fluid collections in the patient group ranged between 0.37 and 3.05×10^{-3} mm^2/s with a median value of 0.85×10^{-3} mm^2/s (Table 2, Fig. 1). Thirteen of 17 lesions had an ADC value of less than 1.00×10^{-3} mm^2/s with a mean of $(0.69 \pm 0.19) \times 10^{-3}$ mm^2/s (range: 0.37 to 0.88×10^{-3} mm^2/s). Based on a comprehensive reference standard including all clinical and imaging information, 14 (82%) of 17 patients were diagnosed with abscess. The lesions of interest in all 17 patients showed ring enhancement on contrast-enhanced T1w imaging. Using an ADC cut-off value of $<1.0 \times 10^{-3}$ mm^2/s for purulent fluid collection, DWI correctly detected 13 (93%) of 14 confirmed cases. Three patients with surgically confirmed non-suppurative fluid collections showed ADC values higher than 1.00×10^{-3} mm^2/s in the presence of peripheral contrast enhancement and were diagnosed with super-infected chronic soft-tissue seroma (ADC 1.84×10^{-3}

mm^2/s, patient 2), synovitis and joint effusion secondary to operatively treated knee joint empyema (ADC 2.15 $\times 10^{-3}$ mm^2/s, patient 5) and an intra-abdominal non-purulent encapsulated fluid collection (ADC 3.05 $\times 10^{-3}$ mm^2/s, patient 15). Patient 3 with severe coxarthritis, osteomyelitis and large periarticular fluid collections showed high ADC values of 1.8 $\times 10^{-3}$ mm^2/s in the presence of strong peripheral contrast enhancement. Abscess was confirmed with ultrasonography-guided abscess puncture and aspiration of pus. The specimen was tested positive for mycobacterium tuberculosis. This patient is to be counted as false-negative, based on an ADC cut-off $<1.0 \times 10^{-3}$ mm^2/s.

Combining the patients and controls, the sensitivity and specificity for abscess were 100% and 85% with contrast-enhanced T1w imaging (diagnostic criterion: ring-enhancing fluid collection) and 93% and 100% with DWI (diagnostic criterion: ADC cut-off $<1.0 \times 10^{-3}$ mm^2/s), respectively. No false-positive results occurred in control subjects. ROC analysis showed an area under the curve of 0.996 for ADC ($P<0.001$). Based on the ROC, using an ADC cut-off of 2.0 $\times 10^{-3}$ mm^2/s would result in a sensitivity of 100% and a specificity of 95% in our study.

Discussion

The results of our study provide evidence that diffusion-weighted MRI is a valuable supplement to conventional MR imaging, or even an alternative to contrast-enhanced T1w MRI, in young patients with suspected abdominal and soft-tissue abscess.

These findings correlate well with recent reports on detectability of abscess formations on DWI in Crohn's disease,[9] soft tissue abscess,[10,11] intra-orbital abscess formations,[12] prostatic abscess[13] and intracranial abscess[14,15] in adult patients. Mean ADC values for abscess reported in these studies mostly range between 0.6 and 0.8 $\times 10^{-3}$ mm^2/s, while Oto et al[9] reported substantially higher mean ADC values for abdominal abscess and suggested an ADC cut-off value of 2.0 $\times 10^{-3}$ mm^2/s for differentiation between abscess and non-purulent fluid collection. The underlying biochemical and biophysical principles that cause restricted diffusion in abscess formations are not yet fully understood. Available studies on brain abscess suggest that ADC values correlate with the content of viable inflammatory cells within the abscess cavity, rather than pus viscosity or protein content.[14,15] Mishra et al[14] reported no difference in mean ADC between pyogenic and tuberculous brain abscesses. At this point, it remains unclear why one of our patients with tuberculous soft tissue abscess showed less restricted diffusion, compared with other patients. In this particular case, though, the diagnosis of abscess was established with a high level of confidence based on T2w and post-contrast T1w imaging. In two of our patients, detection of abdominal abscess formation within co-existing significant non-purulent free fluid collections would have been difficult, if not impossible, based on the conventional MR sequences alone.

We consider DWI a very helpful tool to localize pathological fluid collections and to differentiate serous fluid collections from abscess. Image fusion with T2w sequences, as shown in Fig. 2, may further facilitate spatial co-location of anatomical background and functional information obtained from DWI. Although infected fluid collections can be diagnosed on post-contrast T1w sequences based on their peripheral wall enhancement, non-suppurative fluid collections adjacent to inflamed soft tissue formations may mimic abscess. As seen in our series, the diagnostic sign of ring enhancement is not completely specific for abscess, so DWI may help the radiologist to distinguish abscess from other fluid collections with more diagnostic confidence and higher specificity. Furthermore, some patients may not receive intravenous contrast agent for a history of allergy or renal failure and may thus be examined with diffusion-weighted MRI as a stand-alone technique.

Our study results demonstrate the feasibility of DWI in pediatric patients and young adults. The free-breathing technique employed in our study yielded diagnostic images with few artifacts and was found to be particularly useful for very young and ill patients who may not be able to sufficiently cooperate with breath-hold techniques. While conventional MRI sequences showed motion artifacts in two of our study patients, no such artifacts were seen on DWI owing to the inherent fast acquisition with echo-planar imaging. Instead, we noted the known proneness to susceptibility artifacts in the head and neck anatomical region.[16] With presently available scanner hardware and software, DWI is still limited in terms of scanning volume and spatial resolution.

Limitations of our study include the relatively small patient group examined on different MR scanners, the variety of abscess manifestations in different anatomical regions and a lack of biochemical analysis of purulent specimen from abscess formations for correlation with ADC. At present, we have got no sufficiently large patient cohort with abscess-mimicking pathologies for comparison, so that the interpretation of our study results is limited to the characterization of purulent and serous fluid collections.

In conclusion, DWI showed high sensitivity and specificity for abdominal and soft-tissue abscess in

this series of pediatric patients. DWI increased the specificity of contrast-enhanced T1w imaging. Further investigations on DWI features of non-abscess ring-enhancing fluid collections, including bilioma, urinoma or hematoma, will further clarify the role of DWI in characterizing intra-abdominal and musculoskelettal fluid collections.

Funding: None.

Ethical approval: Not needed, as the study is based on retrospective analysis of routine imaging data. The anonymized scientific use of such data is covered by the treatment contract signed by the patients.

Competing interest: None.

Contributors: H Neubauer is the guarantor of the presented work. H Neubauer, D Hahn and M Beer conceived, planned and conducted the study. I Platzer, V Mueller, T Meyer, J Liese participated in data acquisition and analysis. H Koestler was responsible for developing MRI sequences. All authors participated in drafting and revising the manuscript and approved the submitted version.

References

1 Schaefer PW, Grant PE, Gonzalez RG. Diffusion-weighted MR imaging of the brain. Radiology 2000;217:331-345.
2 Guzman R, Barth A, Lövblad KO, El-Koussy M, Weis J, Schroth G, et al. Use of diffusion-weighted magnetic resonance imaging in differentiating purulent brain processes from cystic brain tumors. J Neurosurg 2002;97:1101-1107.
3 Koh DM, Collins DJ. Diffusion-weighted MRI in the body: applications and challenges in oncology. AJR Am J Roentgenol 2007;188:1622-1635.
4 Sun YS, Zhang XP, Tang L, Ji JF, Gu J, Cai Y, et al. Locally advanced rectal carcinoma treated with preoperative chemotherapy and radiation therapy: preliminary analysis of diffusion-weighted MR imaging for early detection of tumor histopathologic downstaging. Radiology 2010;254:170-178.
5 Kwee TC, Takahara T, Luijten PR, Nievelstein RAJ. ADC measurements of lymph nodes: inter- and intra-observer reproducibility study and an overview of the literature. Eur J Radiol 2010;75:215-220.
6 Kiryu S, Dodanuki K, Takao H, Watanabe M, Inoue Y, Takazoe M, et al. Free-breathing diffusion-weighted imaging for the assessment of inflammatory activity in Crohn's disease. J Magn Reson Imaging 2009;29:880-886.
7 Kwee TC, Takahara T, Vermoolen MA, Bierings MB, Mali WP, Nievelstein RA. Whole-body diffusion-weighted imaging for staging malignant lymphoma in children. Pediatr Radiol 2010;40:1592-1602.
8 MacKenzie JD, Gonzalez L, Hernandez A, Ruppert K, Jaramillo D. Diffusion-weighted and diffusion tensor imaging for pediatric musculoskeletal disorders. Pediatr Radiol 2007;37:781-788.
9 Oto A, Schmid-Tannwald C, Agrawal G, Kayhan A, Lakadamyali H, Orrin S, et al. Diffusion-weighted MR imaging of abdominopelvic abscesses. Emerg Radiol 2011;18:515-524.
10 Unal O, Koparan HI, Avcu S, Kalender AM, Kisli E. The diagnostic value of diffusion-weighted magnetic resonance imaging in soft tissue abscesses. Eur J Radiol 2009;77:490-494.
11 Harish S, Chiavaras MM, Kotnis N, Rebello R. MR imaging of skeletal soft tissue infection: utility of diffusion-weighted imaging in detecting abscess formation. Skeletal Radiol 2011;40:285-294.
12 Sepahdari AR, Aakalu VK, Kapur R, Michals EA, Saran N, French A, et al. MRI of orbital cellulitis and orbital abscess: the role of diffusion-weighted imaging. AJR Am J Roentgenol 2009;193:W244-250.
13 Singh P, Yadav MK, Singh SK, Lal A, Khandelwal N. Case series: diffusion weighted MRI appearance in prostatic abscess. Indian J Radiol Imaging 2011;21:46-48.
14 Mishra AM, Gupta RK, Saksena S, Prasad KN, Pandey CM, Rathore D, et al. Biological correlates of diffusivity in brain abscess. Magn Reson Med 2005;54:878-885.
15 Tomar V, Yadav A, Rathore RK, Verma S, Awasthi R, Bharadwaj V, et al. Apparent diffusion coefficient with higher b-value correlates better with viable cell count quantified from the cavity of brain abscess. AJNR Am J Neuroradiol 2011;32:2120-2125.
16 Abdel Razek AA, Gaballa G, Elhawarey G, Megahed AS, Hafez M, Nada N. Characterization of pediatric head and neck masses with diffusion-weighted MR imaging. Eur Radiol 2009;19:201-208.

Received January 5, 2012
Accepted after revision March 7, 2012